Hepatic TRAF2 Regulates Glucose Metabolism Through Enhancing Glucagon Responses

Zheng Chen,[1] Liang Sheng,[1] Hong Shen,[1] Yujun Zhao,[2] Shaomeng Wang,[2] Robert Brink,[3] and Liangyou Rui[1]

Obesity is associated with intrahepatic inflammation that promotes insulin resistance and type 2 diabetes. Tumor necrosis factor receptor–associated factor (TRAF)2 is a key adaptor molecule that is known to mediate proinflammatory cytokine signaling in immune cells; however, its metabolic function remains unclear. We examined the role of hepatic TRAF2 in the regulation of insulin sensitivity and glucose metabolism. TRAF2 was deleted specifically in hepatocytes using the Cre/loxP system. The mutant mice were fed a high-fat diet (HFD) to induce insulin resistance and hyperglycemia. Hepatic glucose production (HGP) was examined using pyruvate tolerance tests, ^{2}H nuclear magnetic resonance spectroscopy, and in vitro HGP assays. The expression of gluconeogenic genes was measured by quantitative real-time PCR. Insulin sensitivity was analyzed using insulin tolerance tests and insulin-stimulated phosphorylation of insulin receptors and Akt. Glucagon action was examined using glucagon tolerance tests and glucagon-stimulated HGP, cAMP-responsive element–binding (CREB) phosphorylation, and expression of gluconeogenic genes in the liver and primary hepatocytes. Hepatocyte-specific TRAF2 knockout (HKO) mice exhibited normal body weight, blood glucose levels, and insulin sensitivity. Under HFD conditions, blood glucose levels were significantly lower (by >30%) in HKO than in control mice. Both insulin signaling and the hypoglycemic response to insulin were similar between HKO and control mice. In contrast, glucagon signaling and the hyperglycemic response to glucagon were severely impaired in HKO mice. In addition, TRAF2 overexpression significantly increased the ability of glucagon or a cAMP analog to stimulate CREB phosphorylation, gluconeogenic gene expression, and HGP in primary hepatocytes. These results suggest that the hepatic TRAF2 cell autonomously promotes hepatic gluconeogenesis by enhancing the hyperglycemic response to glucagon and other factors that increase cAMP levels, thus contributing to hyperglycemia in obesity. ***Diabetes*** **61:566–573, 2012**

Obesity is a primary risk factor for type 2 diabetes. It is associated with chronic inflammation that in turn contributes to insulin resistance. Multiple proinflammatory cytokines, including tumor necrosis factor (TNF)-α, interleukin (IL)-1, and IL-6, impair insulin sensitivity, thereby promoting type 2 diabetes progression (1–4). Chronic inflammation in the liver is believed to contribute to hyperglycemia and glucose intolerance in obesity (2,3). The liver controls blood glucose levels mainly through glycogenolysis and gluconeogenesis. In fasting states, glycogenolysis and gluconeogenesis increase, providing glucose for neurons and erythrocytes that depend on glucose for survival (5,6). Hepatic glucose production (HGP) rates are determined by a balance between insulin and various counterregulatory hormones (e.g., glucagon, glucocorticoids, growth hormone, and catecholamines). Insulin suppresses HGP by inhibiting the expression of rate-limiting gluconeogenic enzymes, including PEPCK and glucose 6-phosphatase (G6Pase), whereas counterregulatory hormones have an opposite effect (6–11). In type 2 diabetes, gluconeogenesis is abnormally elevated, thus contributing to hyperglycemia and glucose intolerance (12). In obesity, the expression of TNF-α, IL-1, and IL-6 is markedly elevated in the liver, and suppression of liver inflammation greatly attenuates insulin resistance, hyperglycemia, and glucose intolerance (2,3,13). Proinflammatory cytokines are believed to impair insulin signaling and the ability of insulin to suppress gluconeogenesis in hepatocytes, thereby contributing to hyperglycemia and glucose intolerance in obesity-associated type 2 diabetes (12,14–16). However, intracellular signaling pathways that mediate cytokine suppression of insulin action in hepatocytes remain largely unclear. In addition, it is unclear whether proinflammatory cytokines regulate the activity of glucagon or other counterregulatory hormones.

TNF receptor–associated factor (TRAF)2 is a TRAF family member and recruited to the TNF receptors or Toll-like receptors upon ligand binding (17,18). It mediates the activation of multiple downstream pathways, including the canonical and noncanonical nuclear factor-κB pathways and the Jun NH_2-terminal kinase (JNK) pathways (17–25). TRAF2 is expressed in multiple tissues, including the liver (26). TRAF2 knockout mice die after birth (27,28), indicating that TRAF2 is required for postnatal growth and development. TRAF2 has been extensively examined in immune cells and is believed to mediate key cytokine responses (17,18,21); however, the function of TRAF2 in metabolic tissues, including the liver, has not been reported.

In this study, we report that hepatic TRAF2 regulates glucagon but not insulin signaling. Hepatocyte-specific deletion of TRAF2 impairs glucagon's ability to stimulate gluconeogenesis, thus protecting against diet-induced hyperglycemia. Therefore, hepatic TRAF2 is involved in inflammation-promoted hyperglycemia in obesity.

RESEARCH DESIGN AND METHODS

$TRAF2^{flox/flox}$ mice were provided by R.B. Albumin-Cre mice were from The Jackson Laboratory (Bar Harbor, ME). Hepatocyte-specific TRAF2 knockout (HKO) mice were generated by crossing $TRAF2^{flox/flox}$ mice with albumin-Cre mice (in C57BL/6 genetic background). Mice were housed on a 12-h light/dark cycle in the Unit for Laboratory Animal Medicine at the University of Michigan. Mice were fed either a normal chow (9% fat; Laboratory Diet) or a high-fat

From the [1]Department of Molecular and Integrative Physiology, University of Michigan Medical School, Ann Arbor, Michigan; the [2]Department of Internal Medicine, University of Michigan Medical School, Ann Arbor, Michigan; and the [3]Garvan Institute of Medical Research, Darlinghurst, New South Wales, Australia.

Corresponding author: Liangyou Rui, ruily@umich.edu.

Received 8 April 2011 and accepted 15 December 2011.

DOI: 10.2337/db11-0474

diet (HFD; 60% fat; Research Diets) ad libitum with free access to water. Animal experiments were conducted following the protocols approved by the University of Michigan Committee on the Use and Care of Animals.

Animal experiments. These experiments were conducted in conscious mice. Blood samples were collected from tail veins, and blood glucose and plasma insulin were measured as described previously (29). Plasma glucagon was measured using glucagon radioimmunoassay kits (LINCO, St. Charles, MO). Glucose tolerance tests (GTTs) and insulin tolerance tests (ITTs) have been described previously (30). In pyruvate tolerance tests, mice were fasted overnight and intraperitoneally injected with sodium pyruvate (2 g/kg body wt). Blood glucose was monitored after pyruvate injection. In GTTs, mice were fasted for 5 h and intraperitoneally injected with glucagon (10 μg/kg body wt). To measure relative contributions of gluconeogenesis and glycogenolysis to hepatic glucose production, mice were fed an HFD for 10–12 weeks, fasted for 24 h, and intraperitoneally injected with deuterium water (99%, 27 mL/kg body wt) (Cambridge Isotope Laboratories, Andover, MA). Blood samples were collected via retro-orbital sinus 30 min after injection and pooled from three mice in each group as described previously (31). The pooled samples were used to purify glucose that was subsequently converted to monoacetone glucose (MAG) (31,32). MAG was subjected to ^{2}H nuclear magnetic resonance (NMR) spectroscopy analysis. ^{2}H NMR spectra were obtained by a 17.6 T Varian spectrometer (Varian Medical Systems, Palo Alto, CA), and relative ^{2}H enrichments in H2, H5, and H6s resonances were measured. The relative contributions of glycogenolysis and gluconeogenesis (glycerol and PEP as substrates) to HGP were calculated as described previously (32–35): glycogenolysis: (H2-H5)/H2; gluconeogenesis (glycerol): (H5-H6s)/H2; gluconeogenesis (PEP): H6s/H2.

Immunoprecipitation and immunoblotting. Mice were fasted 20–24 h, anesthetized, and administrated insulin (2 units/kg body wt) via inferior vena. Livers were isolated and homogenized in a lysis buffer (50 mmol/L Tris HCl, pH 7.5, 1.0% NP-40, 150 mmol/L NaCl, 2 mmol/L EGTA, 1 mmol/L Na_3VO_4, 100 mmol/L NaF, 10 mmol/L $Na_4P_2O_7$, 1 mmol/L phenylmethylsulfonyl fluoride [PMSF], 10 μg/mL aprotinin, and 10 μg/mL leupeptin) as described previously (36,37). Liver extracts were immunoprecipitated with anti–insulin receptor (IR) antibody (Santa Cruz Biotechnology) and immunoblotted with anti–phospho-Tyr antibody (Upstate). Liver extracts were also immunoblotted with antibodies against phospho-Akt (pSer473 from Cell Signaling Technology and Thr308 from Santa Cruz Biotechnology) or total Akt (Santa Cruz Biotechnology).

Immunostaining. Liver frozen sections (7 μm) were fixed in 4% paraformaldehyde for 30 min, blocked with 5% normal goat serum (Invitrogen Life Technologies, Carlsbad, CA) plus 1% BSA for 3 h, and incubated with rat anti-F4/80 antibody (eBioscience, San Diego, CA) at 4°C overnight. F4/80-positive cells were visualized using Cy2-conjugated goat anti-rat secondary antibodies and a fluorescent microscopy.

Quantitative real-time PCR analysis. Total RNAs were extracted using TRIzol reagent (Invitrogen Life Technologies) as described previously (36). The first-strand cDNAs were synthesized using random primers and Maloney murine leukemia virus reverse transcriptase (Promega, Madison, WI). mRNA abundance was measured using ABsolute QPCR SYBR Mix (Thermo Fisher Scientific, Epsom, Surrey, U.K.) and Mx3000P real-time PCR system (Stratagene, La Jolla, CA). The expression of individual genes was normalized to the expression of 36B4, a housekeeping gene. Primers for real-time quantitative PCR (qPCR) include peroxisome proliferator–activated receptor γ coactivator (PGC)-1α-F: TGGACGGAAGCAATTTTTCA, PGC-1α-R: TTACCTGCGCAAGCTTCTCT; PEPCK-F: ATCATCTTTGGTGGCCGTAG, PEPCK-R: ATCTTGCCCTTGTG TTCTGC; G6Pase-F: CCGGTGTTTGAACGTCATCT, G6Pase-R: CAATGCCTGAC AAGACTCCA; 36B4-F: AAGCGCGTCCTGGCATTGTCT, 36B4-R: CCGCAGGGG CAGCAGTGGT; IL-1β-F: GCCTTGGGCCTCAAAGGAAAGAATC, IL-1β-R: GGAAG ACACAGATTCCATGGTGAAG; IL-6-F: AGCCAGAGTCCTTCAGA, IL-6-R: GGTCC TTAGCCACTCCT; and TNF-α-F: CATCTTCTCAAAATTCGAGTGACAA, TNF-α-R: TGGGAGTAGACAAGGTACAACCC.

Primary hepatocyte cultures, adenoviral infection, and HGP assays. Primary hepatocyte cultures were prepared by liver perfusion with type II collagenase (Worthington Biochemical, Lakewood, NJ) and grown on collagen-coated plates as described previously (37). The cells were infected with indicated adenoviruses and subjected to HGP assays 16 h after infection as described previously (38). In brief, primary hepatocytes were incubated for 4 h in Krebs-Ringer bicarbonate buffer (118 mmol/L NaCl, 2.5 mmol/L $CaCl_2$, 4.8 mmol/L KCl, 25 mmol/L $NaHCO_3$, 1.1 mmol/L KH_2PO_4, 1.2 mmol/L $MgSO_4$, 10 μg $ZnSO_4$, 0.6% BSA, and 10 mmol/L HEPES, pH 7.4) supplemented with 10 mmol/L lactate and 1 mmol/L pyruvate, in the presence or absence of glucagon or the mixture of 10 μmol/L N^6,2′-*O*-dibutyryl-cAMP sodium salt (DB-cAMP) and 100 nmol/L dexamethasone. Glucose in culture medium was measured and normalized to total protein levels.

Isolation of Kupffer cell fractions. Livers were perfused with type II collagenase. Dissociated liver cells were filtered through a cell strainer (100 μm) and centrifuged at 50*g* for 2 min. The supernatants were centrifuged at 200*g* for 10 min, and the pellets were resuspended in Ca^{2+}- and Mg^{2+}-free PBS and loaded onto a Percoll gradient solution (40 and 25%). After centrifugation at 500*g* for 20 min, Kupffer cells were highly enriched in the pellets.

G6Pase activity assay. G6Pase activity was measured as described previously (39). Liver samples (~50 mg) were homogenized in an ice-cold lysis buffer (100 mmol/L Tris, pH 7.5, 0.25 mol/L sucrose, 5 mmol/L EDTA, and 1 mmol/L PMSF) and centrifuged at 10,500*g* and 4°C for 20 min. The supernatants were centrifuged at 100,000*g* and 4°C for 60 min. The pellets (microsomal fraction) were resuspended in a buffer (100 mmol/L Na-cacodylate and 10% glycerol, pH 6.5) and protein concentrations were measured. Microsomal fraction (10 μL) was incubated in a reaction buffer (100 mmol/L sodium cacodylate and 46 mmol/L glucose-6-phosphate) for 10 min at 37°C. Reaction was terminated by adding trichloroacetic acid (1.3%) and centrifuged at 16,000*g* for 5 min. The supernatant (10 mL) or phosphorous standards (0, 81.25, 162.5, 325, and 650 μmol/L) was mixed with Taussky-Shorr color reagents (1% ammonium molybdate, 0.5 mol/L sulfuric acid, and 0.18 mol/L ferrous sulfate) and incubated for 5 min at room temperature. Optical absorbance (620 nm) was measured by a SynergyTM HT multimode 96-well plate reader (BioTek) and used to calculate anorganic phosphate concentrations. G6Pase activity was expressed as milliunits (nanamoles of anorganic phosphate released per minute) and normalized to microsomal protein levels (milligrams).

Nuclear extract preparation. Mice were fasted for 3 h, anesthetized, and injected with glucagon (30 μg/kg body wt) via inferior vena. Livers were dissected 5 min after injection and homogenized in a lysis buffer (20 mmol/L HEPES, 1 mmol/L EDTA, 250 mmol/L sucrose, 10 μg/mL aprotinin, 10 μg/mL leupeptin, 1 mmol/L PMSF, 1 mmol/L Na_3VO_3, and 0.5 mmol/L dithiothreitol, pH 7.4). Liver nuclei were isolated by sequential centrifugation at 4°C at 1,100*g* and 4,000*g*, respectively. The pellets were resuspended in a high-salt solution (20 mmol/L HEPES, 420 mmol/L NaCl, 0.2 mmol/L EDTA, 0.5 mmol/L dithiothreitol, 1 mmol/L PMSF, and 1 mmol/L Na_3VO_3, pH 7.9) to prepare nuclear extracts.

Statistical analysis. Data are presented as means ± SEM. Differences between groups were analyzed by two-tailed Student *t* tests. $P < 0.05$ was considered statistically significant.

RESULTS

Hepatocyte-specific deletion of TRAF2 is not sufficient to alter insulin sensitivity and glucose metabolism. TRAF2 mRNA abundance increased in mice with either genetic or dietary obesity (Fig. 1*A*). To determine the metabolic function of liver TRAF2, HKO mice were generated using the Cre/loxP system. TRAF2$^{flox/flox}$ mice were generated and characterized previously (21). HKO mice were generated by crossing TRAF2$^{flox/flox}$ mice with albumin-Cre transgenic mice, and both TRAF2$^{flox/flox}$ and albumin-Cre mice were used as control. As expected, TRAF2 was deleted specifically in the livers but not muscle and adipose tissues of HKO mice (Fig. 1*B*). To verify TRAF2 deletion specifically in hepatocytes but not other types of liver cells, hepatocytes and Kupffer cells were purified and subjected to genotyping and qPCR analysis. The *TRAF2* gene was deleted in the hepatocytes but not Kupffer cells of HKO mice (Fig. 1*C*). TRAF2 mRNA levels were markedly reduced in hepatocytes but not Kupffer cells (Fig. 1*D*). The residual TRAF2 mRNA in the hepatocyte fractions of HKO mice may result from a contamination of other cell types.

To examine the metabolic function of hepatic TRAF2, we measured blood glucose and insulin and performed GTTs and ITTs in mice fed a normal chow. Both overnight fasting blood glucose (Fig. 1*E*) and plasma insulin (data not shown) were similar between HKO and control mice. Glucose clearance rates and the ability of exogenous insulin to reduce blood glucose were also similar between HKO and control mice (Fig. 1*F* and *G*). These results suggest that TRAF2 deficiency in hepatocytes alone is not sufficient to alter glucose metabolism.

Hepatocyte-specific deletion of TRAF2 attenuates diet-induced hyperglycemia. Because inflammation promotes insulin resistance in obesity (13,40), we examined the role of hepatic TRAF2 in obesity-associated metabolic disorders. HKO and control mice were fed an HFD, and

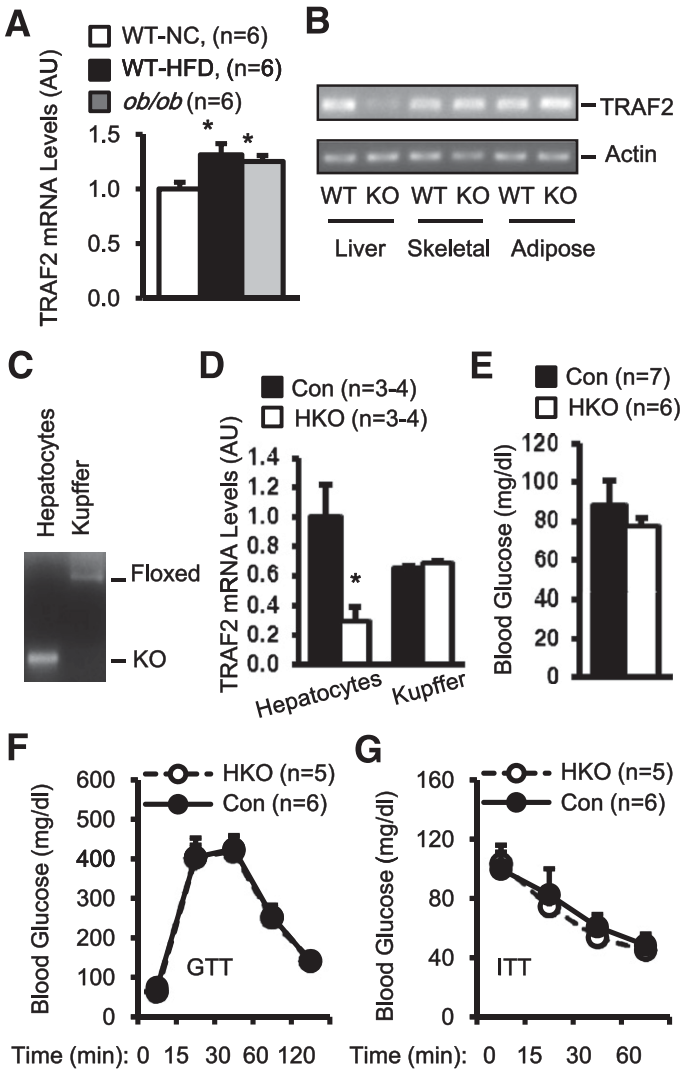

FIG. 1. Hepatic TRAF2 is dispensable for glucose metabolism under normal conditions. *A*: TRAF2 mRNA abundance was measured in the liver by qPCR and normalized to 36B4 mRNA levels. WT-NC, wild-type mice fed a normal chow diet (14 weeks); WT-HFD, WT mice fed an HFD (14 weeks); *ob/ob*, leptin-deficient *ob/ob* mice (14 weeks); AU, arbitrary unit. *B*: Total RNAs were extracted from WT and HKO mice and used to measure TRAF2 transcription by RT-PCR. *C*: Genomic DNA was prepared from purified hepatocytes and Kupffer cells and subjected to PCR-based genotyping analysis. *D*: TRAF2 mRNA abundance was measured in purified hepatocytes and Kupffer cells by qPCR and normalized to 36B4 mRNA levels. *E*: Fasting (overnight) blood glucose levels in HKO and control male mice (23 weeks). *F* and *G*: GTTs (D-glucose: 2 g/kg body wt) and ITTs (1 unit/kg body wt) were performed in HKO and control males at age 22–23 weeks. Data are mean ± SEM. *$P < 0.05$. Con, control.

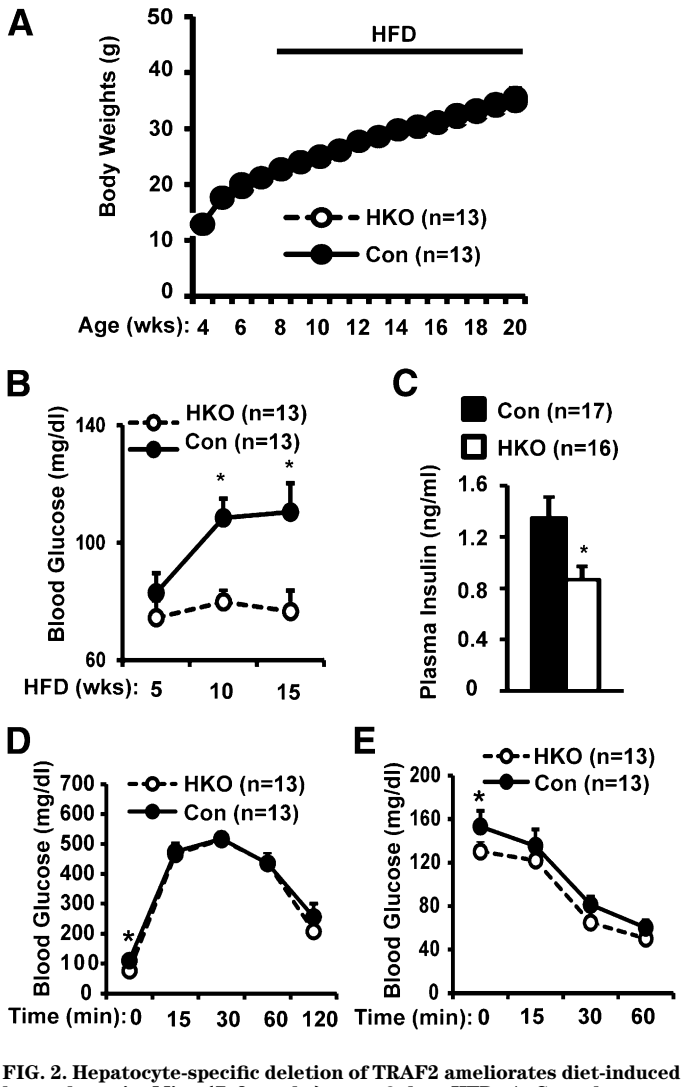

FIG. 2. Hepatocyte-specific deletion of TRAF2 ameliorates diet-induced hyperglycemia. Mice (7–8 weeks) were fed an HFD. *A*: Growth curves. *B*: Fasting (overnight) blood glucose. *C*: Fasting plasma insulin levels in mice fed an HFD for 15 weeks. *D* and *E*: GTTs (D-glucose: 2 g/kg body wt) and ITTs (1 unit/kg body wt) were performed in HKO and control males fed an HFD for 15 and 16 weeks, respectively. Control groups contained both $TRAF2^{flox/flox}$ ($n = 10–14$) and albumin-Cre ($n = 3$) mice. Data are mean ± SEM. *$P < 0.05$. Con, control; Wks, weeks.

blood glucose and plasma insulin were measured. Body weight was similar between HKO and control mice (Fig. 2*A*). Control mice developed hyperglycemia progressively under HFD conditions; in contrast, blood glucose levels were maintained at relatively normal levels in HFD-fed HKO mice (Fig. 2*B*). Fasting blood glucose was 30% lower in HKO than in control mice fed an HFD for 15 weeks (HKO: 76.6 ± 7.0 mg/dL, $n = 13$; Control: 110.5 ± 9.8 mg/dL, $n = 13$; $P = 0.01$). Blood glucose also was reduced (by 22%) in HKO mice under fed conditions (HKO: 111.2 ± 4.6 mg/dL, $n = 10$; Control: 141.1 ± 5.7 mg/dL, $n = 16$; $P = 0.001$). Fasting plasma insulin levels also significantly decreased in HKO mice (Fig. 2*C*). A reduction in plasma insulin may be secondary to decreased blood glucose in HKO mice. These data indicate that hepatic TRAF2 contributes to diet-induced hyperglycemia and hyperinsulinemia in mice.

To further analyze insulin sensitivity and glucose metabolism, we performed GTTs and ITTs. It is surprising that glucose excursion rates were similar between HKO and control mice (Fig. 2*D*), and exogenous insulin similarly reduced blood glucose between these two groups (Fig. 2*E*). These results suggest that hepatic TRAF2 contributes to diet-induced hyperglycemia independently of insulin resistance.

Hepatocyte-specific deletion of TRAF2 decreases hepatic gluconeogenesis. We analyzed HGP using pyruvate tolerance tests. Mice were fed an HFD for 17 weeks and injected with pyruvate, a gluconeogenic substrate. Blood glucose increased in both HKO and control mice after pyruvate injection; however, glucose levels were significantly lower in HKO than in control mice 0, 15, 30, and 120 min after injection, and the area under the curve (AUC) decreased by ~24% in HKO mice (Fig. 3*A*). To measure relative contributions of glycogenolysis and gluconeogenesis to HGP, mice were fasted for 24 h and

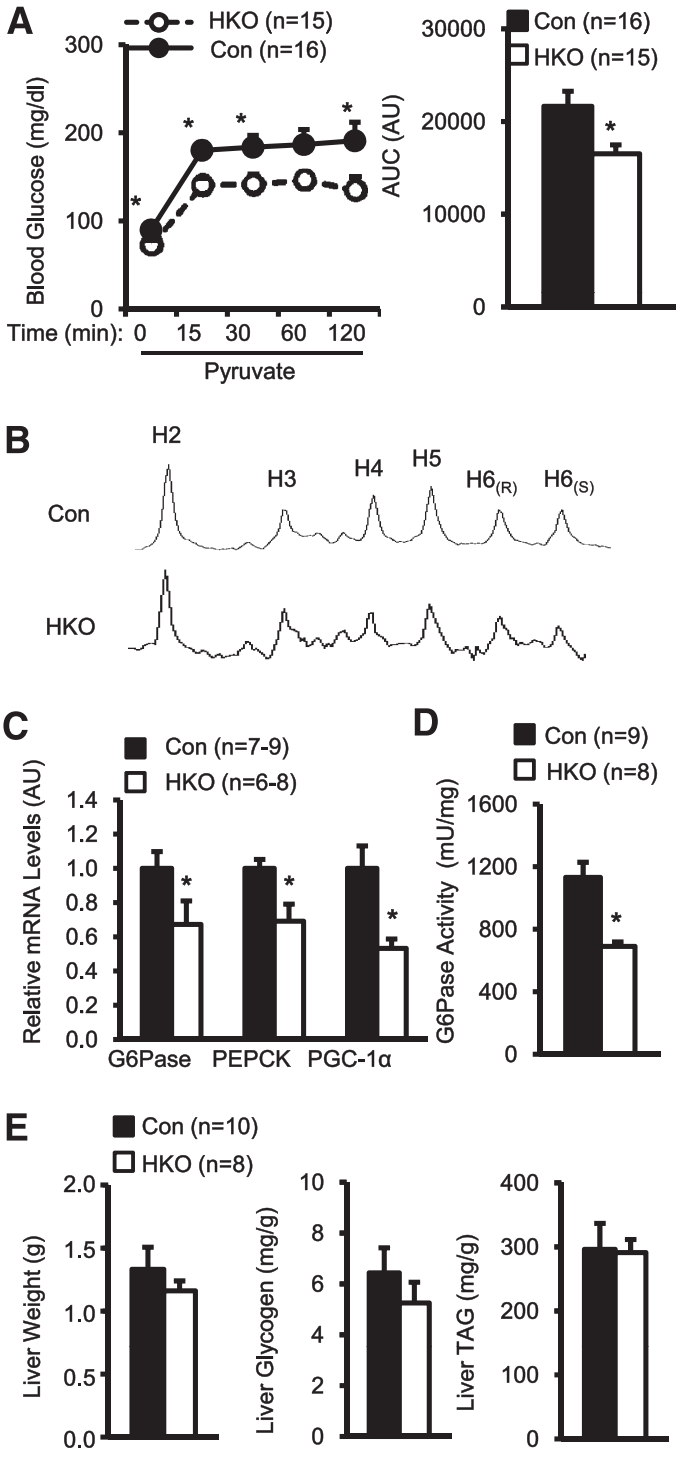

FIG. 3. Hepatocyte-specific deletion of TRAF2 suppresses the hepatic gluconeogenic program under HFD conditions. *A*: HKO and control ($TRAF2^{flox/flox}$; $n = 13$; albumin-Cre: $n = 3$) male mice were fed an HFD for 17 weeks. Mice were fasted for 16 h and intraperitoneally injected with sodium pyruvate (2 g/kg body wt). Blood glucose was monitored after injection, and AUCs were calculated. AU, arbitrary unit. *B*: Mice (7–8 weeks) were fed an HFD for 10–12 weeks and subjected to ^{2}H NMR analysis. ^{2}H NMR spectra of a MAG derived from plasma glucose (pooled from three animals per group) were presented. *C*: HKO and control males were fed an HFD for 18 weeks. Total liver RNAs were extracted and used to measure the mRNA abundance of the indicated genes by qPCR. The expression of these genes was normalized to the expression of 36B4. *D*: HKO and control males were fed an HFD for 18 weeks and fasted for 20–24 h. G6Pase activity was measured in liver microsomal fractions and normalized to microsomal protein levels. *E*: HKO and control males were fed an HFD for 18 weeks, and liver weight, glycogen contents, and triacylglycerol (TAG) levels were measured. Data are mean ± SEM. *$P < 0.05$. Con, control.

intraperitoneally injected with deuterium water. Blood samples were collected 30 min after injection and subjected to ^{2}H NMR analysis to estimate the contributions of glycogenolysis and gluconeogenesis to HGP as described previously (31–35). ^{2}H NMR spectra were different between control and HKO mice (Fig. 3*B*). The fraction of glucose derived from PEP-stimulated gluconeogenesis was markedly reduced in HKO mice (Control: 64.7 ± 7.1%, $n = 9$; HKO: 26.8 ± 8.9%, $n = 9$; $P = 0.029$). In contrast, the fraction of glycogenolysis-derived glucose increased in HKO mice (Control: 10.8 ± 3.2%, $n = 9$; HKO: 29.3 ± 3.4%, $n = 9$; $P = 0.017$). Increased glycogenolysis may be an adaptation to decreased gluconeogenesis in HKO mice.

Plasma lactate levels were similar between control and HKO mice fed an HFD for 18 weeks (HKO: 4.23 ± 0.40 mmol/L, $n = 16$; Control: 5.07 ± 0.56 mmol/L, $n = 16$; $P = 0.22$). These data suggest that the supply of gluconeogenic substrate may not be the determinant factor for reduced gluconeogenesis in HKO mice. To determine whether

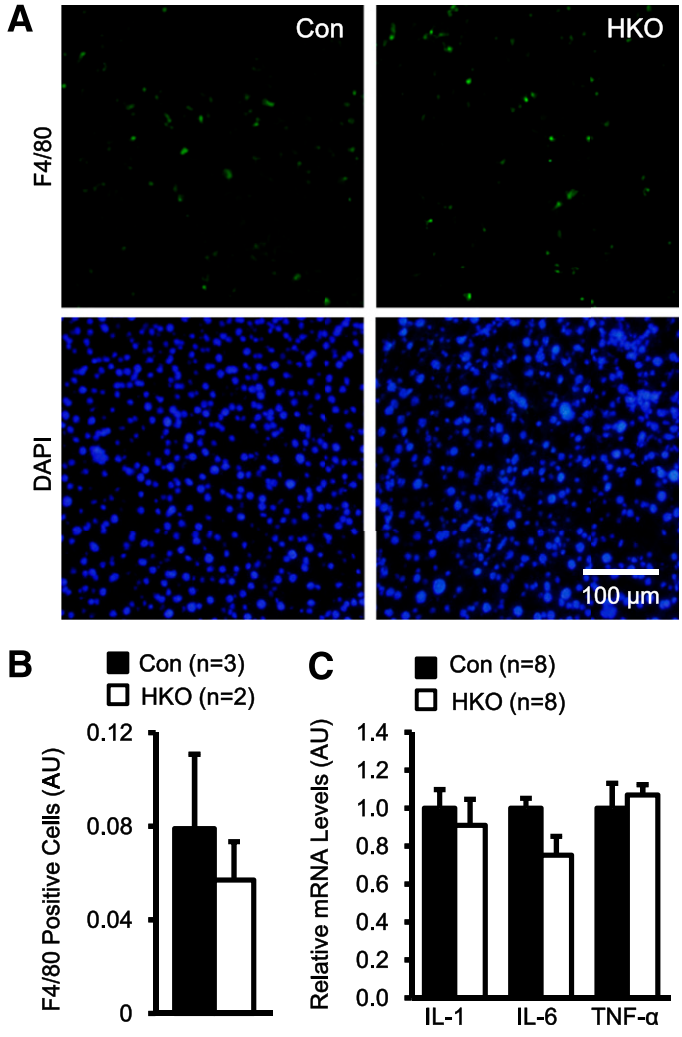

FIG. 4. Hepatocyte-specific deletion of TRAF2 does not ameliorate liver inflammation levels under HFD conditions. HKO and control (Con) males (7–8 weeks) were fed an HFD for 18 weeks. *A*: Liver frozen sections were stained with anti-F4/80 antibody and DAPI. *B*: F4/80-positive cells were accounted and normalized to total cell numbers. AU, arbitrary unit. *C*: Total liver RNAs were extracted and used to measure the mRNA abundance of the indicated genes by qPCR. The expression of these genes was normalized to the expression of 36B4. Data are mean ± SEM. (A high-quality digital representation of this figure is available in the online issue.)

hepatic TRAF2 regulates the hepatic gluconeogenic program, mice were fed an HFD for 18 weeks and fasted for ~20 h. Liver mRNA was extracted and used to measure the mRNA abundance of key gluconeogenic genes by qPCR. The expression of PGC-1α, PEPCK, and G6Pase decreased by 47, 31, and 33% in HKO mice, respectively (Fig. 3*C*). Consistently, liver G6Pase activity was reduced by 39% in HKO mice (Fig. 3*D*). Furthermore, liver weights, glycogen contents, and triacylglycerol levels were also similar between HKO and control mice (Fig. 3*E*). Taken together, these results suggest that under HFD conditions, hepatic TRAF2 directly promotes hepatic gluconeogenesis, thereby contributing to hyperglycemia.

Hepatocyte-specific deletion of TRAF2 does not alter liver inflammation and insulin signaling under HFD conditions. To determine whether hepatocyte-specific deletion of TRAF2 ameliorates HFD-induced liver inflammation, mice were fed an HFD for 18 weeks and liver sections were immunostained with antibodies against F4/80, a Kupffer cell marker. Kupffer cell number was similar between control and HKO mice (Fig. 4*A* and *B*). To further analyze liver inflammation, we measured the expression of proinflammatory cytokines in these mice using qPCR. The expression of liver TNF-α, IL-1, and IL-6 was similar between HKO and control mice (Fig. 4*C*). In addition, plasma levels of alanine aminotransferase, a marker of liver injury, were also similar between HKO and control mice (Control: 93.3 ± 19.1 units/L, n = 5; HKO: 80.8 ± 16.8 units/L, n = 4; P = 0.65). These data indicate that hepatocyte-specific deletion of TRAF2 does not alter the severity of liver inflammation under HFD conditions.

To determine whether hepatic TRAF2 modulates insulin signaling, HKO and control mice were fed a normal chow diet or an HFD for 18 weeks, fasted for 20–24 h, and treated with insulin. Livers were isolated 5 min after insulin treatments to examine insulin signaling pathways. In control mice fed a normal chow diet, insulin rapidly stimulated phosphorylation of Akt (pSer473 and pThr308); as expected, insulin-stimulated Akt phosphorylation was reduced by ~53% (pSer473) and ~36% (pThr308) in mice fed an HFD (Fig. 5*A*). Under HFD conditions, insulin similarly stimulated Tyr phosphorylation of IRs and phosphorylation of Akt (pSer473 and pThr308) in both control and HKO mice (Fig. 5*B*). Therefore, hepatocyte TRAF2 is unlikely to directly regulate insulin signaling. These data raise the possibility that hepatic TRAF2 may regulate HGP through counterregulatory hormones.

Hepatocyte-specific deletion of TRAF2 results in glucagon resistance. Glucagon is a main counterregulatory hormone that stimulates HGP during fasting (6). Plasma glucagon levels increased by 32% in HFD-fed HKO mice (Fig. 6*A*). Hyperglucagonemia is likely to adaptively overcome glucagon resistance in HKO mice. In GTTs, glucagon levels became similar between control and HKO mice 30 min after glucose injection (Control: 89.74 ± 4.16 pg/mL, n = 12; HKO: 103.15 ± 15.02 pg/mL, n = 7; P = 0.3). To examine the hyperglycemic response to glucagon, mice were fed an HFD for 17 weeks and injected with glucagon. Glucagon injection increased plasma glucagon levels by ~10-fold in both control and HKO mice (Control: 1432.34 ± 182.94 pg/mL, n = 3; HKO: 1694.88 ± 556.84 pg/mL, n = 4; P = 0.71). Glucagon markedly increased blood glucose levels in control mice; however, the ability of glucagon to increase blood glucose was severely impaired in HKO mice, and AUC decreased by 25%

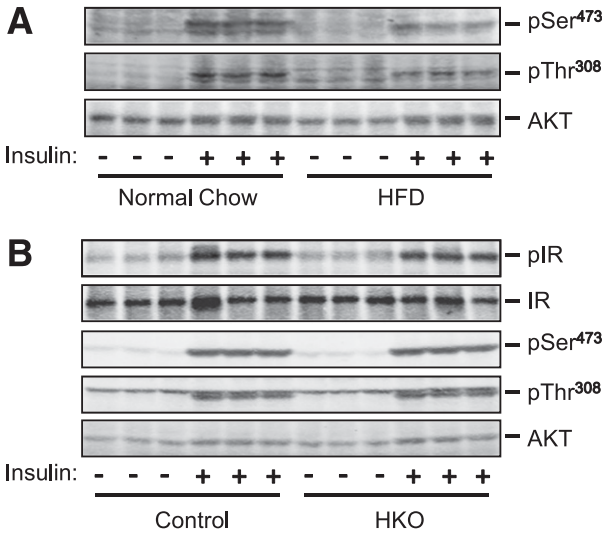

FIG. 5. Hepatocyte-specific deletion of TRAF2 does not alter insulin signaling. *A*: Male mice (7–8 weeks) were fed a normal chow diet or an HFD for an additional 18 weeks. Mice were fasted for 20–24 h, anesthetized, and injected with insulin (2 units/kg body wt) via inferior vena. Liver extracts were prepared 5 min after insulin injection and immunoblotted with antibodies against phospho-Akt (pSer473 or pThr308) or total Akt. *B*: HKO and control mice were fed an HFD for 18 weeks, fasted for 20–24 h, and treated with insulin for 5 min as described above. Liver extracts were immunoblotted with anti–phospho-Akt (pThr308 or pSer473) or anti-Akt antibodies. Liver extracts were also immunoprecipitated with anti-IR and immunoblotted with anti–phospho-Tyr antibody. The blots were reprobed with anti-IR antibody.

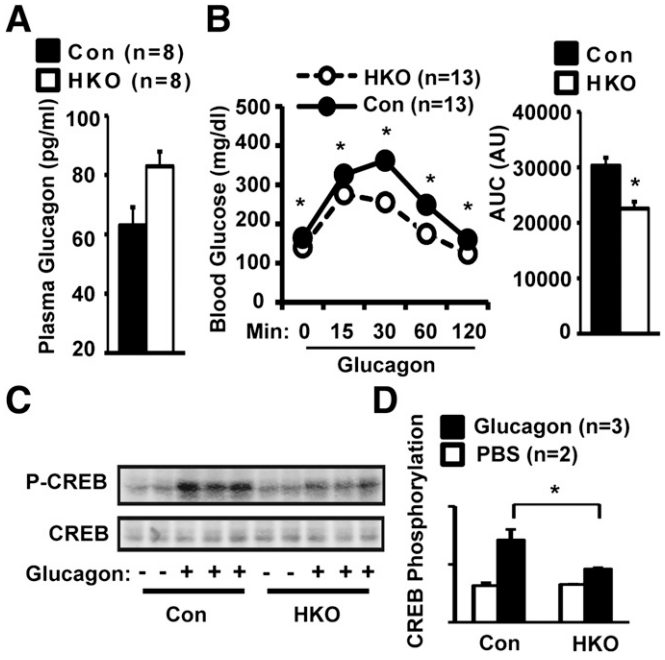

FIG. 6. Hepatocyte-specific deletion of TRAF2 results in glucagon resistance. *A*: Plasma glucagon levels in male mice fed an HFD for 18 weeks. *B*: HKO and control ($TRAF2^{flox/flox}$: n = 10; albumin-Cre: n = 3) males were fed an HFD for 17 weeks. Mice were fasted for 5 h and intraperitoneally injected with glucagon (10 μg/kg body wt). Blood glucose was monitored after injection and AUC was calculated. *C*: HKO and control male mice were fed an HFD for 18 weeks. Mice were fasted for 3 h and injected with glucagon (30 μg/kg body wt) via inferior vena. Liver nuclear extracts were prepared for 5 min after glucagon injection and immunoblotted with anti–phospho-CREB (pSer133) or anti-CREB antibodies. *D*: CREB phosphorylation was quantified using Odyssey software and normalized to total CREB levels. Data are mean ± SEM. *P < 0.05. Con, control; AU, arbitrary unit.

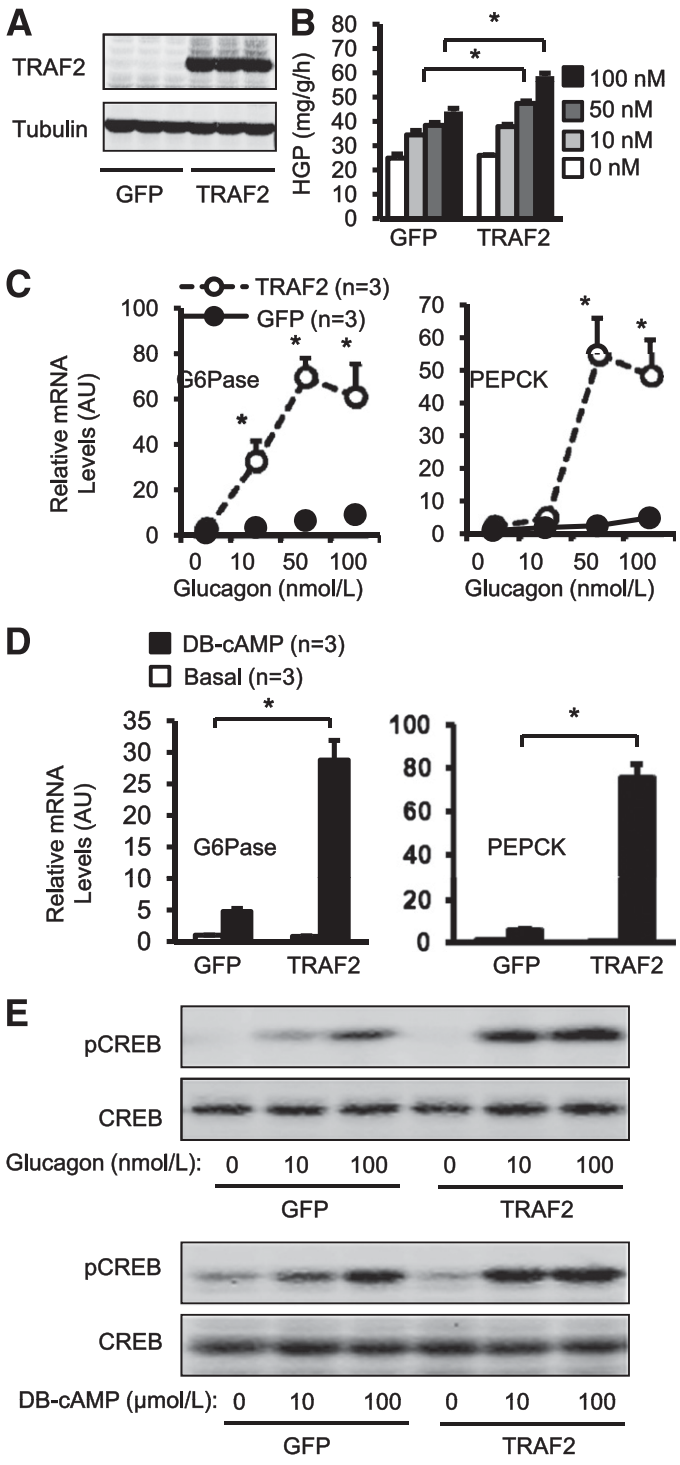

FIG. 7. TRAF2 directly promotes glucose counterregulation in hepatocytes. ***A*****: Primary hepatocyte cultures were isolated from C57BL/6 wild-type mice (10–11 weeks) and infected with GFP or TRAF2 adenoviruses. Cell extracts were prepared 16 h after infection and immunoblotted with antibodies against TRAF2 or tubulin.** ***B*****: Primary hepatocytes were infected with GFP or TRAF2 adenoviruses and treated with glucagon 16 h after infection. HGP was measured 4 h after glucagon stimulation and normalized to total protein levels.** $n = 4$. ***C*****: Primary hepatocytes were infected with GFP or TRAF2 adenoviruses and treated with or without glucagon 16 h after infection. Total RNAs were extracted 2 h after glucagon stimulation and used to measure the mRNA abundance of PEPCK and G6Pase by qPCR. The expression of PEPCK and G6Pase was normalized to 36B4 expression.** ***D*****: Primary hepatocytes were infected with GFP or TRAF2 adenoviruses and treated with DB-cAMP (100 μmol/L for 2 h) 16 h after infection. Total RNAs were extracted and used to measure the mRNA abundance of PEPCK and G6Pase by qPCR.** ***E*****: Primary hepatocytes were coinfected with CREB and GFP or TRAF2 adenoviruses. Sixteen hours after infection, the cells were treated with glucagon or DB-cAMP for 30 min. Cell extracts were immunoblotted with anti–phospho-CREB (pSer133) or anti-CREB antibodies. Data are mean ± SEM. *$P < 0.05$. AU, arbitrary unit.**

(Fig. 6*B*). However, glucagon responses were similar between HKO and control mice fed a normal chow diet (data not shown).

Glucagon, via its G protein–coupled receptors, stimulates cAMP-mediated activation of protein kinase A (6). Protein kinase A phosphorylates cAMP-responsive element–binding (CREB) on Ser133, thereby stimulating CREB transcriptional activity (5,6). CREB in turn activates the transcription of PGC-1α, PEPCK, and G6Pase, key gluconeogenic genes (5,6). To determine whether hepatic TRAF2 modulates glucagon-stimulated CREB phosphorylation, HKO and control mice were fed an HFD for 18 weeks and injected with glucagon. Liver nuclear extracts were prepared 5 min after glucagon injection and immunoblotted with phospho-CREB (pSer133) antibody. Glucagon robustly stimulated CREB phosphorylation in control mice; however, CREB phosphorylation decreased by 35% in HKO mice (Fig. 6*C* and *D*). Total CREB levels were similar between HKO and control mice (Fig. 6*C*). These data suggest that hepatic TRAF2 promotes HGP at least in part by enhancing the hyperglycemic response to glucagon.

TRAF2 directly promotes glucagon action in primary hepatocytes. To determine whether TRAF2 directly promotes HGP, primary hepatocyte cultures were prepared from C57BL/6 mice and infected with TRAF2 or green fluorescent protein (GFP) adenoviruses. Recombinant TRAF2 protein was detected in TRAF2 but not GFP adenovirus–infected cells (Fig. 7*A*). Infected cells were treated with glucagon and subjected to HGP assays. Glucagon dose-dependently stimulated HGP in GFP adenovirus–infected cells; TRAF2 overexpression significantly increased the ability of glucagon (at 50 and 100 nmol/L) to stimulate HGP (Fig. 7*B*). TRAF2 overexpression also increased the ability of DB-cAMP (a cAMP analog) to stimulate HGP by 62% (GFP: 128.24 ± 5.34 mg/g/h, $n = 5$; TRAF2: 208.11 ± 19.92 mg/g/h, $n = 5$; $P = 0.005$). To determine whether TRAF2 directly promotes the hepatic gluconeogenic program, primary hepatocytes were infected with TRAF2 or GFP adenoviruses and treated with glucagon, and the expression of PEPCK and G6Pase was measured by qPCR. Glucagon stimulated G6Pase expression by 343% at 10 nmol/L, 647% at 50 nmol/L, and 907% at 100 nmol/L in GFP adenovirus–infected cells; TRAF2 overexpression further increased glucagon-stimulated G6Pase expression by 11-fold (10 nmol/L glucagon stimulation), 24-fold (50 nmol/L glucagon), and 22-fold (100 nmol/L glucagon) in TRAF2 adenovirus–infected cells (Fig. 7*C*). TRAF2 overexpression similarly enhanced the ability of glucagon to stimulate PEPCK expression in primary hepatocytes (Fig. 7*C*). DB-cAMP also stimulated the expression of PEPCK and G6Pase, and TRAF2 overexpression further increased DB-cAMP–stimulated expression of PEPCK and G6Pase (Fig. 7*D*). To determine whether TRAF2 directly modulates CREB activation, primary hepatocytes were coinfected with CREB and GFP or TRAF2 adenoviruses and treated with glucagon. Glucagon stimulated CREB phosphorylation in a dose-dependent manner, and TRAF2 overexpression further increased glucagon-stimulated CREB phosphorylation (Fig. 7*E*). DB-cAMP also dose-dependently stimulated CREB phosphorylation, and TRAF2 overexpression further increased DB-cAMP–stimulated phosphorylation

of CREB (Fig. 7*E*). These results suggest that hepatic TRAF2 promotes HGP at least in part by increasing glucagon's ability to stimulate phosphorylation of CREB that in turn activates gluconeogenic genes, including *PEPCK* and *G6Pase*.

DISCUSSION

The contribution of inflammation to insulin resistance, hyperglycemia, and glucose intolerance has been extensively examined; however, the intracellular signaling pathways that mediate proinflammatory cytokine-induced insulin resistance and hyperglycemia remain largely unclear. We examined the metabolic function of TRAF2 pathways in hepatocytes. TRAF2 binds to TNF receptor family members as well as Toll-like receptor family members and is believed to mediate the activation of both the canonical inhibitor of κB kinase-β/nuclear factor-κB1 pathway and the JNK pathway (17–19,28,41–44). TRAF2 also mediates endoplasmic reticulum (ER) stress–induced activation of JNK (45,46). ER stress is believed to contribute to insulin resistance and type 2 diabetes progression (40,46–50). It is surprising that deletion of TRAF2 in hepatocytes did not alter insulin signaling in the livers of HKO mice fed either a normal chow diet or an HFD. Exogenous insulin reduced blood glucose to a similar degree in both HKO and control mice, suggesting that hepatic TRAF2 deficiency does not alter systemic insulin sensitivity. A simple explanation of these observations is that hepatocyte TRAF2 pathways do not mediate insulin resistance under inflammation and ER stress conditions. Alternatively, other TRAF family members may have redundant function and compensate for TRAF2 deficiency in hepatocytes.

HKO mice were protected against HFD-induced hyperglycemia. Plasma insulin levels were also lower in HKO than in control mice. Hypoinsulinemia may be secondary to hypoglycemia in HKO mice. Hepatic glucose production, gluconeogenesis, and the expression of key gluconeogenic genes (e.g., PGC-1α, PEPCK, and G6Pase) were significantly decreased in HKO mice fed an HFD. These observations suggest that under HFD conditions, hepatic TRAF2 promotes hepatic gluconeogenesis, thus contributing to hyperglycemia. Moreover, hepatocyte-specific deletion of TRAF2 did not alter the severity of liver inflammation in HFD-fed HKO mice, suggesting that hepatocyte TRAF2 pathways do not mediate HFD-induced liver inflammation. These data also suggest that TRAF2 is able to separately regulate immune responses (by immune cell TRAF2) and metabolic responses (by hepatocyte TRAF2) through mutually independent pathways.

The hepatic gluconeogenic program is controlled by insulin and counterregulatory hormones (5,6). Hepatic TRAF2 appears to regulate gluconeogenesis through glucagon rather than insulin. Hepatocyte-specific deletion of TRAF2 severely impaired the ability of glucagon to increase blood glucose and inhibited glucagon to stimulate CREB phosphorylation in the liver. Furthermore, TRAF2 overexpression directly increased glucagon's ability to stimulate glucose production in primary hepatocytes. TRAF2 overexpression also increased the ability of a cAMP analog to stimulate CREB phosphorylation, the expression of PEPCK and G6Pase, and glucose production in primary hepatocytes. These results suggest that the hepatic TRAF2 cell autonomously increases the ability of glucagon and other cAMP-dependent factors to stimulate the hepatic gluconeogenic program and hepatic glucose production. These observations raise the possibility that hepatic TRAF2 may act downstream of inflammation and/or ER stress to promote the hyperglycemic response to counterregulatory hormones, thereby contributing to hyperglycemia in type 2 diabetes.

In summary, we show that hepatocyte-specific deletion of TRAF2 decreases the hyperglycemic response to glucagon and protects against hyperglycemia and hyperinsulinemia in HKO mice fed an HFD; conversely, TRAF2 overexpression directly increases the ability of glucagon and a cAMP analog to stimulate the expression of gluconeogenic genes and glucose production in primary hepatocytes. TRAF2 deficiency in hepatocytes does not alter insulin signaling in the liver. Thus, hepatic TRAF2 is a previously unknown positive regulator of glucagon action and hepatic gluconeogenesis in overnutrition states.

ACKNOWLEDGMENTS

This study was supported by grants DK-065122 and DK-073601 from the National Institutes of Health (NIH) and by Research Award 1-09-RA-156 from the American Diabetes Association. This work used the cores supported by the Michigan Diabetes Research and Training Center (funded by NIH 5P60-DK-20572), the University of Michigan Cancer Center (funded by NIH 5P30-CA-46592), the University of Michigan Nathan Shock Center (funded by NIH P30-AG-013283), and the University of Michigan Gut Peptide Research Center (funded by NIH DK-34933).

No potential conflicts of interest relevant to this article were reported.

Z.C. and L.R. researched data and wrote, reviewed, and edited the manuscript. L.S., H.S., Y.Z., S.W., and R.B. researched data, contributed to discussion, and reviewed and edited the manuscript. L.R. is the guarantor of this article.

The authors thank Dr. Eugenio Alvarado (Department of Chemistry, University of Michigan) for his assistance in NMR experiments and Drs. Haoran Su, Lin Jiang, and Kae Won Cho (Department of Molecular and Integrative Physiology, University of Michigan Medical School) for their assistance and discussion.

REFERENCES

1. Uysal KT, Wiesbrock SM, Marino MW, Hotamisligil GS. Protection from obesity-induced insulin resistance in mice lacking TNF-alpha function. Nature 1997;389:610–614
2. Cai D, Yuan M, Frantz DF, et al. Local and systemic insulin resistance resulting from hepatic activation of IKK-beta and NF-kappaB. Nat Med 2005;11:183–190
3. Arkan MC, Hevener AL, Greten FR, et al. IKK-beta links inflammation to obesity-induced insulin resistance. Nat Med 2005;11:191–198
4. Yuan M, Konstantopoulos N, Lee J, et al. Reversal of obesity- and diet-induced insulin resistance with salicylates or targeted disruption of Ikkbeta. Science 2001;293:1673–1677
5. Ali S, Drucker DJ. Benefits and limitations of reducing glucagon action for the treatment of type 2 diabetes. Am J Physiol Endocrinol Metab 2009;296: E415–E421
6. Jiang G, Zhang BB. Glucagon and regulation of glucose metabolism. Am J Physiol Endocrinol Metab 2003;284:E671–E678
7. Gonzalez GA, Montminy MR. Cyclic AMP stimulates somatostatin gene transcription by phosphorylation of CREB at serine 133. Cell 1989;59:675–680
8. Herzig S, Long F, Jhala US, et al. CREB regulates hepatic gluconeogenesis through the coactivator PGC-1. Nature 2001;413:179–183
9. Koo SH, Flechner L, Qi L, et al. The CREB coactivator TORC2 is a key regulator of fasting glucose metabolism. Nature 2005;437:1109–1111
10. Postic C, Dentin R, Girard J. Role of the liver in the control of carbohydrate and lipid homeostasis. Diabetes Metab 2004;30:398–408
11. Zhou XY, Shibusawa N, Naik K, et al. Insulin regulation of hepatic gluconeogenesis through phosphorylation of CREB-binding protein. Nat Med 2004;10:633–637

12. Biddinger SB, Kahn CR. From mice to men: insights into the insulin resistance syndromes. Annu Rev Physiol 2006;68:123–158
13. Shoelson SE, Goldfine AB. Getting away from glucose: fanning the flames of obesity-induced inflammation. Nat Med 2009;15:373–374
14. Baron AD, Schaeffer L, Shragg P, Kolterman OG. Role of hyperglucagonemia in maintenance of increased rates of hepatic glucose output in type II diabetics. Diabetes 1987;36:274–283
15. Basu A, Shah P, Nielsen M, Basu R, Rizza RA. Effects of type 2 diabetes on the regulation of hepatic glucose metabolism. J Investig Med 2004;52:366–374
16. Dinneen S, Alzaid A, Turk D, Rizza R. Failure of glucagon suppression contributes to postprandial hyperglycaemia in IDDM. Diabetologia 1995;38:337–343
17. Napolitano G, Karin M. Sphingolipids: the oil on the TRAFire that promotes inflammation. Sci Signal 2010;3:pe34
18. Xia ZP, Chen ZJ. TRAF2: a double-edged sword? Sci STKE 2005;2005:pe7
19. Devin A, Cook A, Lin Y, Rodriguez Y, Kelliher M, Liu Z. The distinct roles of TRAF2 and RIP in IKK activation by TNF-R1: TRAF2 recruits IKK to TNF-R1 while RIP mediates IKK activation. Immunity 2000;12:419–429
20. Gardam S, Sierro F, Basten A, Mackay F, Brink R. TRAF2 and TRAF3 signal adapters act cooperatively to control the maturation and survival signals delivered to B cells by the BAFF receptor. Immunity 2008;28:391–401
21. Grech AP, Amesbury M, Chan T, Gardam S, Basten A, Brink R. TRAF2 differentially regulates the canonical and noncanonical pathways of NF-kappaB activation in mature B cells. Immunity 2004;21:629–642
22. He L, Grammer AC, Wu X, Lipsky PE. TRAF3 forms heterotrimers with TRAF2 and modulates its ability to mediate NF-kappaB activation. J Biol Chem 2004;279:55855–55865
23. Hsu H, Shu HB, Pan MG, Goeddel DV. TRADD-TRAF2 and TRADD-FADD interactions define two distinct TNF receptor 1 signal transduction pathways. Cell 1996;84:299–308
24. Vallabhapurapu S, Matsuzawa A, Zhang W, et al. Nonredundant and complementary functions of TRAF2 and TRAF3 in a ubiquitination cascade that activates NIK-dependent alternative NF-kappaB signaling. Nat Immunol 2008;9:1364–1370
25. Zarnegar BJ, Wang Y, Mahoney DJ, et al. Noncanonical NF-kappaB activation requires coordinated assembly of a regulatory complex of the adaptors cIAP1, cIAP2, TRAF2 and TRAF3 and the kinase NIK. Nat Immunol 2008;9:1371–1378
26. Zapata JM, Krajewska M, Krajewski S, et al. TNFR-associated factor family protein expression in normal tissues and lymphoid malignancies. J Immunol 2000;165:5084–5096
27. Yeh WC, Shahinian A, Speiser D, et al. Early lethality, functional NF-kappaB activation, and increased sensitivity to TNF-induced cell death in TRAF2-deficient mice. Immunity 1997;7:715–725
28. Nguyen LT, Duncan GS, Mirtsos C, et al. TRAF2 deficiency results in hyperactivity of certain TNFR1 signals and impairment of CD40-mediated responses. Immunity 1999;11:379–389
29. Ren D, Li M, Duan C, Rui L. Identification of SH2-B as a key regulator of leptin sensitivity, energy balance, and body weight in mice. Cell Metab 2005;2:95–104
30. Duan C, Yang H, White MF, Rui L. Disruption of the SH2-B gene causes age-dependent insulin resistance and glucose intolerance. Mol Cell Biol 2004;24:7435–7443
31. Burgess SC, Jeffrey FM, Storey C, et al. Effect of murine strain on metabolic pathways of glucose production after brief or prolonged fasting. Am J Physiol Endocrinol Metab 2005;289:E53–E61
32. Burgess SC, Weis B, Jones JG, et al. Noninvasive evaluation of liver metabolism by 2H and ^{13}C NMR isotopomer analysis of human urine. Anal Biochem 2003;312:228–234
33. Hausler N, Browning J, Merritt M, et al. Effects of insulin and cytosolic redox state on glucose production pathways in the isolated perfused mouse liver measured by integrated 2H and ^{13}C NMR. Biochem J 2006;394:465–473
34. Schumann WC, Gastaldelli A, Chandramouli V, et al. Determination of the enrichment of the hydrogen bound to carbon 5 of glucose on 2H2O administration. Anal Biochem 2001;297:195–197
35. Landau BR, Wahren J, Chandramouli V, Schumann WC, Ekberg K, Kalhan SC. Contributions of gluconeogenesis to glucose production in the fasted state. J Clin Invest 1996;98:378–385
36. Ren D, Zhou Y, Morris D, Li M, Li Z, Rui L. Neuronal SH2B1 is essential for controlling energy and glucose homeostasis. J Clin Invest 2007;117:397–406
37. Zhou Y, Jiang L, Rui L. Identification of MUP1 as a regulator for glucose and lipid metabolism in mice. J Biol Chem 2009;284:11152–11159
38. Cho KW, Zhou Y, Sheng L, Rui L. Lipocalin-13 regulates glucose metabolism by both insulin-dependent and insulin-independent mechanisms. Mol Cell Biol 2011;31:450–457
39. Schmutz I, Ripperger JA, Baeriswyl-Aebischer S, Albrecht U. The mammalian clock component PERIOD2 coordinates circadian output by interaction with nuclear receptors. Genes Dev 2010;24:345–357
40. Hotamisligil GS. Endoplasmic reticulum stress and inflammation in obesity and type 2 diabetes. Novartis Found Symp 2007;286:86–94; discussion 94–88, 162–163, 196–203
41. Song HY, Régnier CH, Kirschning CJ, Goeddel DV, Rothe M. Tumor necrosis factor (TNF)-mediated kinase cascades: bifurcation of nuclear factor-kappaB and c-jun N-terminal kinase (JNK/SAPK) pathways at TNF receptor-associated factor 2. Proc Natl Acad Sci U S A 1997;94:9792–9796
42. Matsuzawa A, Tseng PH, Vallabhapurapu S, et al. Essential cytoplasmic translocation of a cytokine receptor-assembled signaling complex. Science 2008;321:663–668
43. Ea CK, Deng L, Xia ZP, Pineda G, Chen ZJ. Activation of IKK by TNFalpha requires site-specific ubiquitination of RIP1 and polyubiquitin binding by NEMO. Mol Cell 2006;22:245–257
44. Karin M, Gallagher E. TNFR signaling: ubiquitin-conjugated TRAFfic signals control stop-and-go for MAPK signaling complexes. Immunol Rev 2009;228:225–240
45. Urano F, Wang X, Bertolotti A, et al. Coupling of stress in the ER to activation of JNK protein kinases by transmembrane protein kinase IRE1. Science 2000;287:664–666
46. Ozcan U, Cao Q, Yilmaz E, et al. Endoplasmic reticulum stress links obesity, insulin action, and type 2 diabetes. Science 2004;306:457–461
47. Aguirre V, Uchida T, Yenush L, Davis R, White MF. The c-Jun NH(2)-terminal kinase promotes insulin resistance during association with insulin receptor substrate-1 and phosphorylation of Ser(307). J Biol Chem 2000;275:9047–9054
48. Lee YH, Giraud J, Davis RJ, White MF. c-Jun N-terminal kinase (JNK) mediates feedback inhibition of the insulin signaling cascade. J Biol Chem 2003;278:2896–2902
49. Hirosumi J, Tuncman G, Chang L, et al. A central role for JNK in obesity and insulin resistance. Nature 2002;420:333–336
50. Wang Y, Vera L, Fischer WH, Montminy M. The CREB coactivator CRTC2 links hepatic ER stress and fasting gluconeogenesis. Nature 2009;460:534–537